CHEMICAL ENGINEERING TRANSACTIONS
VOL. 121, 2025
A publication of AIDIC
The Italian Association of Chemical Engineering
Online at www.cetjournal.it
Guest Editors: Petar S. Varbanov

ISBN 979-12-81206-22-9; **ISSN** 2283-9216
DOI: 10.3303/CET25121030

Facilitated by Surface Stabilizers in the Synthesis of ZnSe:Ag Nanocrystals

Thi-Diem Bui *, Trong Tang Nguyen

Faculty of Chemical Engineering, Industrial University of Ho Chi Minh City, 12 Nguyen Van Bao, Hanh Thong ward, Ho Chi Minh City, Vietnam
buithidiem@iuh.edu.vn

In this work, we used surface stabilizers such thioglycolic acid (TGA), polyethylene glycol (PEG), and starch to create nano-sized ZnSe:Ag particles in a non-toxic aqueous solvent. These surface stabilizers aid in stabilizing the nanoparticles' surface by preventing agglomeration and passivation. The structure of ZnSe:5%Ag nanocrystals (NCs) is cubic. Changing the surface stabilizer and doping with Ag metal does not change the structure of the ZnSe substrate material, but it does enhance the fluorescence efficiency by 1.7% to 2.4%. The fluorescence efficiency of ZnSe:5%Ag NCs using PEG stabilizer (ZnSe:5%Ag PEG) was higher than (41,81%) that of NCs using starch stabilizer (33,27%) and higher than that of Ncs using TGA stabilizer (30,54%). Initial assessment of ZnSe:5%Ag PEG NCs for possible biomedical uses.

1. Introduction

Scientists have focused their research on semiconductor nanocrystals in recent decades because to their distinct features when compared to bulk semiconductors (Van *et al.*, 2020). Specifically, group II–VI semiconductor Ncs are high quantum efficiency semiconductors with a straight band gap (Van *et al.*, 2020). One of the most chemically stable and non-toxic (Cd-free) II-VI semiconductors is ZnSe NCs. Because of its exceptional optical and electrical characteristics (Vempuluru *et al.*, 2024), (Zhao *et al.*, 2024), ZnSe offers a wide range of possible uses, such as energy storage, chemical sensors (Mao, 2018), light-emitting devices, solar cells, biomedicine, and photocatalysis.(El-assar *et al.*, 2023; Zahra *et al.*, 2024). However, due to differences in configuration between Zn and Se, ZnSe has defects (Zn belongs to group IIB, Se to group VIA), resulting in low fluorescence efficiency. Furthermore, the suspension bonds on the surface of NCs produce trap states, which alter the fluorescence and quantum efficiency of nanoparticles (Yu *et al.*, 2019). Furthermore, II-VI semiconductor NCs are unstable aggregates or can aggregate extremely quickly due to the lack of a trapping medium, some type of packing, or the particles' uncontrolled development (Winiarz *et al.*, 1999). Surface passivation has a significant impact on nanoparticle optoelectronic properties, and stabilizer binding enhances surface state (Lee et al., 2006). In general, steric hindrances and electrostatic stability can keep nanoparticles from aggregating. As a result, stabilizers are used during nanocrystal manufacturing to maintain particle shape and size while also allowing nanocrystals to expand in volume and surface area. To retain the structural features of the generated NCs, numerous capping agents such as thiophenol, thiourea (Huamg et al., 2006) and glutathione (GSH) (Raievska *et al.*, 2020) have been explored for semiconductor fabrication (Operamolla et al., 2017). However, they are poisonous and hazardous to the environment.
Therefore, it is vital to develop green methods. In this study, we studied nontoxic surface stabilizers with diverse structures: The first ingredient is starch (Castro *et al.*, 2005). Starch is a branched-chain structure made up of two basic components: Amylose and Amylopectin. The ratio of Amylose to Amylopectin has a substantial impact on starch properties. Amylose is a linear polysaccharide made up of glucose units held together by α-1,4-glycosidic linkages. Furthermore, several studies have revealed that this polysaccharide has biomedical applications, such as a substrate for cell spreading, a structure for tissue engineering, a drug delivery system, and an implant. Amylopectin shares the same backbone structure as amylose, but has more α-1,6-linked branch points. This polymer is highly biocompatible and readily biodegradable (Villwock and BeMiller, 2022). Because

Paper Received: 16 June 2025; Revised: 19 September 2025; Accepted: 02 December 2025
Please cite this article as: Biu T.-D., Nguyen T.T., 2025, Facilitated by Surface Stabilizers in the Synthesis of ZnSe:Ag Nanocrystals, Chemical Engineering Transactions, 121, 175-180 DOI:10.3303/CET25121030

of these properties, starch is frequently employed in a variety of biomedical applications, including topical skin administration (Lane, 2011) and degradable drug microspheres. The second option is PEG. PEG is a long linear polyether chain that can absorb water and establish hydrogen bonds, allowing for solubility in polar solvents and stabilizing the colloid under acidic or basic pH conditions (Gamucci *et al.*, 2014). PEG is a low-toxicity polymer, with biocompatibility suitable for medical applications, good water solubility, and exceptionally low immunogenicity and antigenicity (Dreborg and Akerblom, 1990), PEG is a non-biodegradable polymer that is easily removed when exposed to living beings. Its presence in aqueous solution has no adverse effect on protein structure or enzyme activity (Yamaoka et al., 1994). When injected into animals, PEG maintains excellent blood compartment stability while collecting minimally in the liver and spleen. Furthermore, PEG has form flexibility and high water binding properties (Torchilin *et al.*, 1994). As a result, this type of polymer is generally accepted for biological applications. Finally, thioglycolic acid (TGA) has a short linear chain structure, and the hydrophilic carboxylic groups on the outer surface provide good water solubility for NCs after the thiol groups interact with the nanoparticles on their surface.

In this study, we investigated the green synthesis of ZnSe:5%Ag NCs using water as a solvent and non-toxic Zn at low temperature (80-100°C). We used low-toxicity surfactants with different structures such as TGA (short linear chain), PEG (long linear chain), and Starch (linear and branched chain) to investigate the influence of surfactants on the properties and applicability of NCs for detecting *E.coli O157:H7* and *Methicillin-resistant Staphylococcus aureus (MRSA*) bacteria.

2. Experiment

2.1 Materials

High-purity chemical reagents are used for the synthesis of ZnSe NCs and their doped counterparts. Zinc acetate dihydrate ($Zn(CH_3COO)_2 \cdot 2H_2O$, Merck) was used as the Zn precursor, and sodium borohydride ($NaBH_4$, Merck) serves to synthesize. The doping metals silver nitrate ($AgNO_3$, Merck) were introduced in controlled amounts to achieve the desired doping concentration, thioglycolic acid (TGA, Sigma-Aldrich), polyethylene glycol (PEG, Sigma-Aldrich), Starch (Sigma-Aldrich) was employed as a stabilizing agent to enhance the solubility and stability of NCs in aqueous media. Ammonium hydroxide (NH_4OH, Merck) was used to adjust the pH of the reaction mixture to ensure the optimal conditions for NCs formation. Deionized (DI) water was used throughout the synthesis process to maintain the purity of the samples.

2.2 Synthesis of ZnSe:5%Ag NCs with TGA (or PEG, Starch) surface stabilizer

In a 250-mL flask, combine 50 mL of 0.1 N TGA (or PEG, Starch) surface stabilizer, 90 mL of water, 10 mL of 0.1 M Zn^{2+} and 5 mL of 0.01 M Ag^{+}. Whisk the mixture for fifteen minutes. Next, 2 M NH_4OH was added to increase the pH to 7. After adding the combined solution to the NaHSe (which is made from Se powder, $NaBH_4$, and water under vacuum). Weigh 0.40 g of Se and 0.45 g of $NaBH_4$ into the reaction vessel, then remove all air from the flask. Quickly add 5 mL of distilled water to the reaction vessel. The reaction happens instantly, generating a clear solution that yields the NaHSe solution. The solution was kept at 90°C for three hours. Throughout the synthesis process, N_2 gas is continuously introduced into the reaction system to remove O_2 from the vessel. The mixture was cooled, matured for a full day at room temperature, and stored for future research.

2.3 Applications of ZnSe:5%Ag in Biomedicine

The toxicity of ZnSe:5%Ag was studied on *E.coli O157:H7* and *MRSA*. Bacteria were grown overnight on a specified liquid medium before being diluted in saline to gradually diminish the concentration. Bacterial strains were distributed at varying doses in 6mm diameter holes on agar plates. 20mm of NCs solution was placed into each well and incubated at 37°C for 24 hours.

3. Results and discussion

3.1 Structured research and Optical properties

The XRD analysis (*Figure 3.1a)* of ZnSe: 5%Ag TGA, ZnSe: 5%Ag PEG, and ZnSe: 5%Ag NC starch synthesized with different surface stabilizers and doping with Ag metal reveals a cubic crystal structure (zinc blende) when compared to the standard spectrum (Qiao *et al.*, 2019). The diffraction peaks at positions 27.35°, 45.27°, and 54.05° correspond to planes (111), (220), and (311) in accordance with the standard card JCPDS 012-6803. The XRD data show no diffraction patterns for Ag metals or silver compounds. As a result, it is reasonable to believe that Ag was successfully absorbed into ZnSe without causing structural changes. Ag^{+} ions can partially replace Zn^{2+} ions or flow through network cracks. The entire breadth at half maximum peak width of ZnSe:5%Ag PEG results in sharper, taller, and narrower XRD peaks than ZnSe:5%Ag TGA and

ZnSe:5%Ag Starch. This demonstrates that ZnSe:5%Ag PEG has a stable, flawless crystal structure with fewer flaws, more regular, tidy, and uniform crystals than ZnSe:5%Ag TGA and ZnSe:5%Ag Starch

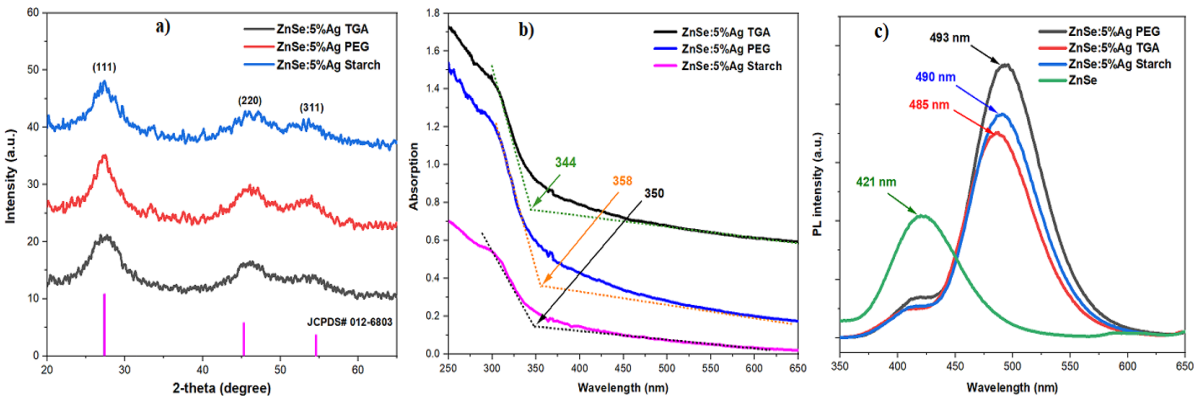

Figure 3.1: a) The XRD results, b) UV-Vis spectra and c) PL spectrum of ZnSe, ZnSe:5%Ag TGA, ZnSe:5%Ag PEG, ZnSe:5%Ag Starch NCs synthesized using different surface stabilizers

The UV-Vis spectra of ZnSe:5%Ag TGA NCs, ZnSe:5%Ag PEG NCs, and ZnSe:5%Ag Starch NCs (Figure 3.1b) revealed that the absorption edge of ZnSe:5%Ag PEG NCs was slightly shifted to longer wavelengths when compared to ZnSe:5%Ag TGA NCs and ZnSe:5%Ag Starch NCs synthesized under the same conditions. This showed that ZnSe:5%Ag PEG NCs were larger than ZnSe:5%Ag TGA and ZnSe:5%Ag Starch nanocrystals. Figure 3.1c shows the PL spectrum of ZnSe:5%Ag nanocrystals synthesized using different surface stabilizers. The peak at 421 nm is the bangap of ZnSe (Califano et al., 2005), whereas the $^1S_o \rightarrow {}^3D_1$ transition of the Ag^+ bright center is the peak at roughly 493 nm.

The luminescence intensity at the Ag^+ core at around 490 nm has a significant impact on the luminescence properties of NCs. The fluorescence efficiency of ZnSe:5%Ag NCs exceeds that of ZnSe. This can be explained by the following factors: Because of configurational deviations in ZnSe (Zn belongs to group IIB, Se to group VIA), the structure contains certain flaws, resulting in a low fluorescence effectiveness for these nanoparticles. Doping with Ag metal improves the fluorescence intensity of NCs. The fluorescence efficiency of ZnSe:5%Ag PEG NCs exceeds that of ZnSe:5%Ag Starch NCs and ZnSe:5%Ag TGA NCs. Because TGA has a short linear structure, it must cover two metal atom sites with its carboxylate group in order to achieve a desirable hexagonal shape. This coordinating capacity allows TGA to absorb free metal ions in the surrounding environment, accelerating crystal formation and negatively impacting nanoparticle optical characteristics. In ZnSe:5%Ag PEG NCs, PEG is a polyether chain that can absorb water and establish hydrogen bonds, allowing for solubility in polar solvents and stabilizing the colloid in acidic or basic pH conditions (Gamucci *et al.*, 2014). PEG molecules are long, straight chains (zigzags). However, when PEG dissolves in water, it forms pentacyclic rings (denutural geometry). A significant quantity of activated oxygen resides in the PEG molecular chain, resulting in strong contacts between PEG molecules and metal ions, particularly transition metal ions, PEG functions as a shell (He *et al.*, 2008). Because of the unique structure of PEG, it functions as a shell, a barrier encircling the nanocrystalline core that limits the carriers trapped on the surface, potentially increasing quantum efficiency. Starch forms a straight chain with lengthy branches. Amylopectin in starch is a branching polysaccharide. The main chain has α-1,4-glycosidic links, while branch chains are linked by α-1,6-glycosidic linkages. Amylopectin's complicated structure includes α-1,6-glycosidic bonds every 20-30 glucose units, resulting in a branch chain. The second level branch chain is generated from the first level branch chain. The Amylopectin molecule branches at several levels (Peng and Perlin, 1987) and surrounds the nanoparticle, reducing the excitation energy of the Ag^+ luminous center. The fluorescence efficiency of NCs synthesized using surface stabilizers when using Rhodamine B as a standard with a fluorescence efficiency of 65% changed in the order: ZnSe:5%Ag PEG (41,81%) > ZnSe:5%Ag Starch (33,27%) > ZnSe:5%Ag TGA (30,54%) > ZnSe (17,73%).

3.2 Study of composition and shape

The presence of PEG on the nanoparticle crystals' surface was determined using FT-IR spectroscopy. Figure 3.3.a depicts the FT-IR spectra of PEG and the representative sample ZnSe:5%Ag PEG NCs, which reveal that the stretching vibration peaks around 3400 cm^{-1} are characteristic of the O-H bond. The vibration peaks at the wave number and 1600 cm^{-1} are typical vibrations of the H-O-H bond of water molecules adsorbed on the material surface (Chmangui *et al.*, 2019). The vibration peaks at 2850 cm^{-1} and 1460 cm^{-1} are typical vibrations

of the -C-H bond in the polyethylene section. The vibration peaks at wave numbers 1100 cm^{-1} and 1150 cm^{-1} are characteristic of the -C-O-C bond. The vibration maxima at 930 cm^{-1} and 825 cm^{-1} are indicative of the -C-O-C bond. The vibration peak at 1700 cm^{-1} is indicative of the carbonyl group (-C=O) (Damiani *et al.*, 2012). The vibration peak at 500 cm^{-1} is characteristic of the Zn-O bond, indicating that there is a connection between Zn in the nanoparticle and oxygen in PEG (Nagaraju *et al.*, 2017). At the same time, PEG has peaks -OH, -CH, -C-O-C, and -C=O. This demonstrates that there is a link between NCs and PEG. This allows NCs to spread well in water, making them more suitable for biological applications. We conclude that PEG was coated on the surface of NCs particles (Tavakkoli Yaraki *et al.*, 2017).

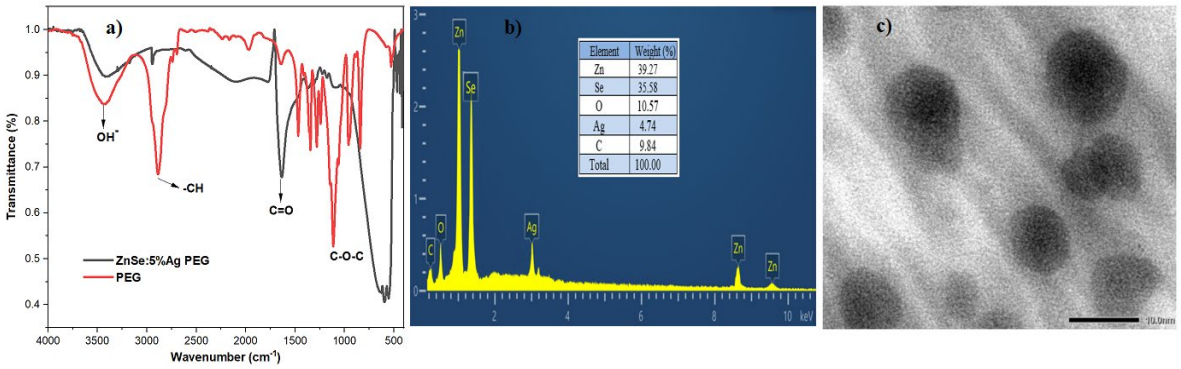

Figure 3.2: a) FT-IR spectrum, b) EDX spectra and c) TEM of ZnSe:5%Ag PEG NCs produced with PEG surface stabilizers.

To determine the presence and ratio of elements in the samples, we examined their EDX spectrum (Figure 3.2b). The presence of Zn, Se, and the doped metal Ag in the samples is plainly visible, with recognizable peaks at the appropriate energies. PEG contains the elements C and O, which have been bound to the surface of the NCs. However, the actual value of the Ag^{+}/Zn^{2+} element ratio is always less than the theoretical value, indicating that there are still a significant number of metal ions that cannot replace Zn^{2+} ions and are removed during sample cleaning. Furthermore, several extraneous elements do not appear in the spectrum image, demonstrating the great purity of the produced ZnSe:5%Ag PEG NCs. The shape of ZnSe:5%Ag PEG NCs is shown in Figure 3.2c. The nanoparticles are nearly spherical in shape with high uniformity. The particle size is relatively uniform, estimated at about 10 nm. The particle size distribution is quite narrow, indicating that the synthesis process is well controlled. No agglomeration was observed, the particles were well dispersed. There was no sign of contamination or unwanted crystallization.

3.3 Study of composition and shape

After synthesizing luminous nanoparticles and examining the effect of surface stabilizers on NC properties, we selected the sample with the best optical properties, ZnSe:5%Ag PEG NCs, to assess the usefulness of NCs in biomedicine. Bacteria were used to distribute the test concentration on agar plates with 6 mm diameter pores. Incubate the well with 20 ml of NCs solution for 24 hours at 37°C. The antibacterial efficacy of ZnSe:5%Ag NCs was evaluated on *E.coli* (Gram-negative) and *MRSA* (Methicillin-resistant Staphylococcus aureus, Gram-positive) bacteria, as shown in Figure 3.3.

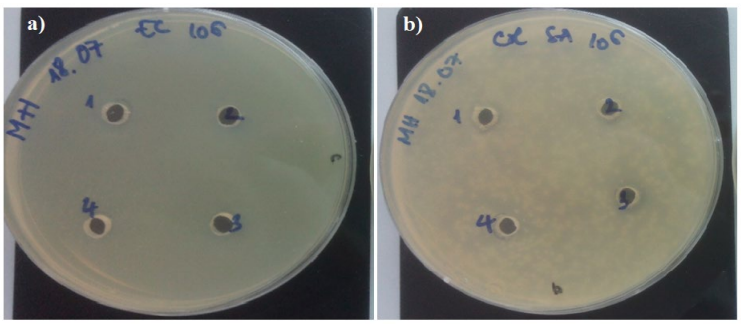

Figure 3.3: Interaction results between NC and E. coli O157:H7 bacteria a), MRSA bacterium b) at doses of 10^{6} CFU/ml (10^{o}, 10^{-1}, 10^{-2}, 10^{-3}), named 1, 2, 3, 4 samples

Both bacterial strains did not exhibit any visible inhibition zones around the four wells marked 1, 2, 3, 4 corresponding to the initial concentrations of ZnSe:5%Ag NCs at 10^{o} (sample 1) and diluted NC solutions at 10^{-1} (sample 2), 10^{-2} (sample 3), and 10^{-3} (sample 4). Bacteria filled the entire agar surface. At the four locations where the four-well sample containing ZnSe:5%Ag NCs was placed, no sterile zones were formed, no halos or reduction in surrounding bacterial density were observed, no repulsion was observed, and the uniform growth of bacteria on the agar surface demonstrated that, under the current experimental conditions, ZnSe:5%Ag NCs had very little effect on the growth of *E.coli* (Figure 3.3a) and *MRSA* (Figure 3.3b). These data show that PEG ZnSe:5%Ag NCs could be useful in biomedical applications.

4. Conclusion

We effectively manufactured ZnSe:5%Ag nanoparticles using surface stabilizers such as TGA (short linear chain), PEG (long chain), and Stacrh (linear and branched chains). ZnSe:5%Ag NCs have a zinc-blend structure, are spherical in shape, well diffused in water, and do not contain toxic group A elements (Cd, Hg, and Pb). Changing surface stabilizers does not alter the topology of the ZnSe network, but it does increase the fluorescence efficiency of the nanoparticles. The fluorescence efficiency of ZnSe: 5%Ag PEG was higher than that of ZnSe: 5%Ag Starch and higher than that of ZnSe: 5%Ag TGA. The ZnSe:5%Ag PEG particles were initially tested and shown to be non-toxic to E.coli and MRSA bacteria. The study's findings could be useful in the production of nanomaterials with non-toxic materials, in environmentally friendly and clean manufacturing techniques, and in expanding the range of applications for nanomaterials in the biomedical industry.

References

Califano, M., Franceschetti, A., & Zunger, A. (2005). Temperature Dependence of Excitonic Radiative Decay in CdSe Quantum Dots: The Role of Surface Hole Traps. Nano Letters, 5(12), 2360–2364. https://doi.org/10.1021/nl051027p

Castro, J. V., Dumas, C., Chiou, H., Fitzgerald, M. A., & Gilbert, R. G. (2005). Mechanistic Information from Analysis of Molecular Weight Distributions of Starch. Biomacromolecules, 6(4), 2248–2259. https://doi.org/10.1021/bm0500401

Chmangui, A., Driss, M. R., Touil, S., Bermejo-Barrera, P., Bouabdallah, S., & Moreda-Piñeiro, A. (2019). Aflatoxins screening in non-dairy beverages by Mn-doped ZnS quantum dots – Molecularly imprinted polymer fluorescent probe. Talanta, 199, 65–71. https://doi.org/10.1016/j.talanta.2019.02.057

Xiaoqun M., (2018). Design of New Electrochemical Sensors and Detection Application of Chemical Feedstock Residues, Chemical Engineering Transactions, 65, 205-210. https://doi.org/10.3303/CET1865035

Damiani, D., Litynski, J. T., McIlvried, H. G., Vikara, D. M., & Srivastava, R. D. (2012b). The US Department of Energy's R&D program to reduce greenhouse gas emissions through beneficial uses of carbon dioxide. Greenhouse Gases: Science and Technology, 2(1), 9–16. https://doi.org/10.1002/ghg

Dreborg, S., & Akerblom, E. B. (1990). Immunotherapy with monomethoxypolyethylene glycol modified allergens. Critical Reviews in Therapeutic Drug Carrier Systems, 6(4), 315–365.

El-assar, M., Taha, T. E., El-Samie, F. E. A., Fayed, H. A., & Aly, M. H. (2023). ZnSe-based highly-sensitive SPR biosensor for detection of different cancer cells and urine glucose levels. In Optical and Quantum Electronics (Vol. 55, Issue 1). Springer. https://doi.org/10.1007/s11082-022-04326-y

Gamucci, O., Bertero, A., Gagliardi, M., & Bardi, G. (2014). Biomedical Nanoparticles: Overview of Their Surface Immune-Compatibility. Coatings, 4(1), 139–159. https://doi.org/10.3390/coatings4010139

He, Y., Lu, H., Sai, L., Su, Y., Hu, M., Fan, C., Huang, W., & Wang, L. (2008). Microwave Synthesis of Water-Dispersed CdTe/CdS/ZnS Core-Shell-Shell Quantum Dots with Excellent Photostability and Biocompatibility. Advanced Materials, 20(18), 3416–3421. https://doi.org/10.1002/adma.200701166

Huang, F., Peng, Y., & Lin, C. (2006). Synthesis and Characterization of ZnS: Ag Nanocrystals Surface-capped with Thiourea1. Chemical Research in Chinese Universities, 22(6), 675–678. https://doi.org/10.1016/S1005-9040(06)60188-8

Lane, M. E. (2011). Nanoparticles and the skin – applications and limitations. Journal of Microencapsulation, 28(8), 709–716. https://doi.org/10.3109/02652048.2011.599440

Lee, Y.-J., Kim, T.-G., & Sung, Y.-M. (2006). Lattice distortion and luminescence of CdSe/ZnSe nanocrystals. Nanotechnology, 17(14), 3539–3542. https://doi.org/10.1088/0957-4484/17/14/030

Nagaraju, G., Udayabhanu, Shivaraj, Prashanth, S. A., Shastri, M., Yathish, K. V., Anupama, C., & Rangappa, D. (2017). Electrochemical heavy metal detection, photocatalytic, photoluminescence, biodiesel production and antibacterial activities of Ag–ZnO nanomaterial. Materials Research Bulletin, 94, 54–63. https://doi.org/10.1016/j.materresbull.2017.05.043

Operamolla, A., Punzi, A., & Farinola, G. M. (2017). Synthetic Routes to Thiol-Functionalized Organic Semiconductors for Molecular and Organic Electronics. Asian Journal of Organic Chemistry, 6(2), 120–138. https://doi.org/10.1002/ajoc.201600460

Peng, Q.-J., & Perlin, A. S. (1987). Observations on N.M.R. spectra of starches in dimethyl sulfoxide, iodine-complexing, and solvation in water-di-methyl sulfoxide. Carbohydrate Research, 160, 57–72. https://doi.org/10.1016/0008-6215(87)80303-8

Qiao, F., Kang, R., Liang, Q., Cai, Y., Bian, J., & Hou, X. (2019). Tunability in the Optical and Electronic Properties of ZnSe Microspheres via Ag and Mn Doping. ACS Omega, 4(7), 12271–12277. https://doi.org/10.1021/acsomega.9b01539

Raievska, O., Stroyuk, O., Dzhagan, V., Solonenko, D., & Zahn, D. R. T. (2020). Ultra-small aqueous glutathione-capped Ag–In–Se quantum dots: luminescence and vibrational properties. RSC Advances, 10(69), 42178–42193. https://doi.org/10.1039/D0RA07706B

Tavakkoli Yaraki, M., Tayebi, M., Ahmadieh, M., Tahriri, M., Vashaee, D., & Tayebi, L. (2017). Synthesis and optical properties of cysteamine-capped ZnS quantum dots for aflatoxin quantification. Journal of Alloys and Compounds, 690, 749–758. https://doi.org/10.1016/j.jallcom.2016.08.158

Torchilin, V. P., Omelyanenko, V. G., Papisov, M. I., Bogdanov, A. A., Trubetskoy, V. S., Herron, J. N., & Gentry, C. A. (1994). Poly(ethylene glycol) on the liposome surface: on the mechanism of polymer-coated liposome longevity. Biochimica et Biophysica Acta (BBA) - Biomembranes, 1195(1), 11–20. https://doi.org/10.1016/0005-2736(94)90003-5

Van, H. T., Vinh, N. D., Ca, N. X., Hien, N. T., Luyen, N. T., Do, P. V., & Khien, N. V. (2020). Effects of ligand and chemical affinity of S and Se precursors on the shape, structure and optical properties of ternary CdS1−xSex alloy nanocrystals. Materials Letters, 264, 127387. https://doi.org/10.1016/j.matlet.2020.127387

Vempuluru, N. R., Kwon, H., Parnapalle, R., Urupalli, B., Munnelli, N., Lee, Y., Marappan, S., Mohan, S., Murikinati, M. K., Muthukonda Venkatakrishnan, S., Kim, K., Ahn, C. W., & Yang, J.-M. (2024). ZnS/ZnSe heterojunction photocatalyst for augmented hydrogen production: Experimental and theoretical insights. International Journal of Hydrogen Energy, 51, 524–539. https://doi.org/10.1016/j.ijhydene.2023.08.249

Villwock, K., & BeMiller, J. N. (2022). The Architecture, Nature, and Mystery of Starch Granules. Part 2. Starch - Stärke, 74(11–12). https://doi.org/10.1002/star.202100184

Winiarz, J. G., Zhang, L., Lal, M., Friend, C. S., & Prasad, P. N. (1999). Photogeneration, charge transport, and photoconductivity of a novel PVK/CdS-nanocrystal polymer composite. Chemical Physics, 245(1–3), 417–428. https://doi.org/10.1016/S0301-0104(99)00057-9

Yamaoka, T., Tabata, Y., & Ikada, Y. (1994). Distribution and Tissue Uptake of Poly(ethylene glycol) with Different Molecular Weights after Intravenous Administration to Mice. Journal of Pharmaceutical Sciences, 83(4), 601–606. https://doi.org/10.1002/jps.2600830432

Yu, J. H., Kim, J., Hyeon, T., & Yang, J. (2019). Facile synthesis of manganese (II)-doped ZnSe nanocrystals with controlled dimensionality. The Journal of Chemical Physics, 151(24). https://doi.org/10.1063/1.5128511

Zahra, T., Alanazi, M. M., Alahmari, S. D., Abdelmohsen, S. A. M., Abdullah, M., Aman, S., Al-Sehemi, A. G., Henaish, A. M. A., Ahmad, Z., & Tahir Farid, H. M. (2024). Hydrothermally synthesized ZnSe@FeSe nanocomposite: A promising candidate for energy storage devices. International Journal of Hydrogen Energy, 59, 97–106. https://doi.org/10.1016/j.ijhydene.2024.01.293

Zhao, Y., Yang, C., Zhang, S., Sun, G., Zhu, B., Wang, L., & Zhang, J. (2024). Investigating the charge transfer mechanism of ZnSe QD/COF S-scheme photocatalyst for H2O2 production by using femtosecond transient absorption spectroscopy. Chinese Journal of Catalysis, 63, 258–269. https://doi.org/10.1016/S1872-2067(24)60069-0.